MECHANISMS OF TRANSPARENT EXOPOLYMER PARTICLES (TEPs) FOULING ON ULTRA-FILTRATION AND ITS REDUCTION BY PVDF/N-TiO_2 HFM

A Thesis

presented to

the Faculty of the Graduate School

at the University of Missouri-Columbia

In Partial Fulfillment

of the Requirements for the Degree

Master of Science

By

ZHIBIAO LI

Dr. Baolin Deng, Thesis Supervisor

July 2014

The undersigned, appointed by the Dean of the Graduate School, have examined the thesis entitled

MECHANISMS OF TRANSPARENT EXOPOLYMER PARTICLES (TEPs) FOULING ON ULTRA-FILTRATION AND ITS REDUCTION BY PVDF/N-TiO_2 HFM

presented by Zhibiao Li,

a candidate for the degree of master of science,

and hereby certify that, in their opinion, it is worthy of acceptance.

_____

Dr. Baolin Deng

_____

Dr. Hao Li

_____

Dr. Paul Chan

ACKNOWLEDGEMENTS

First of all I would like to express my thanks to my advisor Dr. Baolin Deng, a professor in the Department of Chemical Engineering and Department of Civil and Environmental Engineering, for his patience in guiding my research, and all the efforts and encouragement from him all through my studies.

I am also grateful to Dr. Paul Chan in Department of Chemical Engineering and Dr. Hao Li from Department of Mechanical & Aerospace Engineering for being my thesis defense committee members, I am thankful for their suggestions and help in revising my work. Also I would like to thank them for being my teachers of Principle of Chemical Engineering and Nanomaterials courses, repectively, and offering me a life long learning experience.

We greatly thank Dr. Zhiqiang Hu in Department of Civil and Environmental Engineering for offering us the access to zeta sizer, and Dr. Qingsong Yu in the Department of Mechanical & Aerospace Engineering for providing us the contact angle measurement characterization technique.

I would like to extend my thanks to Weiming Hu for generously offerring me *chlorella vulgaris* algal culture and their nutritious solutions which were among the most important materials used in my research.

In addition, I really appreciate Jun Yin, Peng Wan, Zhengyang Wang, and Xiaofeng Wang in helping me fabricate membranes and carry out the characterizations, their help and encouragement means a lot to me.

The financial support for this project is partially provided by the USGS through Missouri Water Resources Research Center.

Last but not least, I would like to express my special thanks and love to my parents for their financial and moral supports, their encouragement means a lot to me throughout my studies in the United States.

TABLE OF CONTENTS

LIST OF TABLES

LIST OF FIGURES

LIST OF ABBREVIATIONS

TEPs	Transparent exopolymer particles
HFM	Hollow fiber membrane
N	Nitrogen
PVDF	Polyvinylidene fluoride
SEM	Scanning electron microscopy
NOM	Natural organic matter
EPS	Extracellular polymeric substance
c-TEPs	Colloidal transparent exopolymer particles
p-TEP	Particulate transparent exopolymer particles
TMP	Transmembrane pressure
MF	Microfiltration
UF	Ultrafiltration
NF	Nanofiltration
RO	Revers osmosis
PES	Polyether sulfone

CA	Cellulose acetate
PS	Polysulfone
PAN	Polyacrylonitrile
PVC	Polyvinylchloride
CNT	Carbon nanotube
UV	Ultraviolet
PVP	Polyvinylpyrrolidone
DMAc	N, N-Dimethylacetamide
DI	Deionized
NPs	Nanoparticles

ABSTRACT

A critical issue for water treatment by membrane process is membrane fouling, which will result in rising hydraulic resistance, decreasing water permeability, and subsquenlty increasing the energy consumption and maintenance cost. Research was carried out on the mechanisms of membrane fouling. Among a variety of foulants, transparent exopolymer particles (TEPs), which play an important role in biofilm formation and membrane fouling, have been overlooked for many years due to their invisiblility.

Here TEPs were first separated from *Chlorella Vulgaris* culture broth and quantified via Alcian Blue staining method as reported in the literature. Other characterizations included particle-size-distribution and zeta potential measurements.

Then the fouling characteristics of ultrafiltration membranes by TEPs were assessed. The fabricated and tested hollow fiber membranes included conventional polyvinylidene fluoride membrane (PVDF) and mixed matrix membranes with titanium dioxide (PVDF/P25) or nitrogen doped titanium dioxide (PVDF/N-TiO_2) nanoparticles integrated into the PVDF matrix. Membranes were characterized by scanning electron microscopy (SEM) and fouling resistance evaluations were performed under dark or visible light irradiation conditions for comparison. The results demonstrated that rejections of TEPs by PVDF, PVDF/P25 and PVDF/N-TiO_2 membrane were all above 85%, although the rejections by PVDF/P25 and PVDF/TiO_2 membranes were about 7% and 10% lower than conventional PVDF membrane respectively. A significant

enhancement of fouling resistance was observed for PVDF/N-TiO_2 membrane under visible light irradiation. The addition of TiO_2 nanoparticles into the PVDF matrix apparently improved the membrane surface hydrophilicity and performance. Additionally, the TiO_2 nanoparticles could be activated under light, and thus contributed to the enhanced anti-fouling properties of the membrane.

CHAPTER 1. INTRODUCTION

1.1 Membrane processes

With the increase of domestic and industrial water consumption, reduction of energy source, and serious environmental pollution problem, membrane technology has been developed as an competitive alternative to distillation for desalination due to its low energy consumption, and simple and safe operation.

Membrane processes have received much attention in recent years, and many materials have been explored for membrane fabrication such as ceramics and metals that are inorganic in nature, organic polymers, and inorganic/organic composite materials. Polymeric membranes can be classified as spiral wound, flat, tubular and hollow fiber according to their configurations. Different membrane processes have different driving forces including temperature and pressure (Mukiibi 2009). Pressure-driven membranes are widely used, especially in drinking water treatment. Generally, there are four types of pressure-driven membrane processes, namely, microfiltration (MF), ultrafiltration (UF), nanofiltration (NF) and reverse osmosis (RO), among which, MF and UF belongs to low pressure processes and the other two are high pressure processes (Guo, Wyart et al. 2010). The characteristics and applications scienarios for each types listed in Table 1.

Table 1. Categorization of membrane processes and their main applications (Rosdianah Ramli and Yasser 2002).

Particulars	Microfiltration (MF)	Ultrafiltration (UF)	Nanofiltration (NF)	Reverse Osmosis (RO)
Pore size	10nm~1μm	3~10nm	2~5nm	Not detectable
Retain particulates (MW)	>300,000	1,000~300,000	>150	<350
Applied pressure	0.005~0.2MPa	0.01~0.3MPa	0.3~1.5MPa	1~10MPa
Main applications	Removal of particles and bacteria, pretreatment for RO and UF	Home water purifiers, fruit juice clarification, drinking water production	Removal of microcontaminants, desalination of brackish water, concentration of chemicals	Desalination of brackish and seawater, production of ultrapure water

Overall many types of membranes have been developed, with each type being suitable for specific types of application. For example, MF and UF membranes are good for particulate removal and have often been used as a pre-treatment for NF/RO processes, while the latters are primiarilay for desalination and removal of soluble organic matters. In the membrane separation system, there is no chemical addition in general, however, membrane fouling could occur and its cleaning process may necessitate the use of cleaning agents

1.2 Overview of UF process and hollow fiber membranes

This research focuses on UF processes using hollow fiber configuration. Hollow fiber membrane processes possess many advantages including easy backwash, compact design and high tolerant to colloidals, but they are sensitive to pressure changes.

Ultrafiltration processes, which can be based on flat sheet or hollow fiber membranes, are most widely applied in water treatment industry, since they can provide

an excellent barrier to contaminants such as colloids, high molecular weight molecules and bacteria. UF treatments are effective in removal of particulate contaminants.

The use of hollow fiber for ultrafiltration is often desired because the driven force and energy requirement for maintaining a constant flux for hollow fiber is much lower than that for other UF configurations (Kennedy, Kamanyi et al. 2008).

Many factors may affect the performance of hollow fiber membranes. The factors belong to three main groups: properties related to the contaminants, properties related to the hollow fiber membrane, and the operating conditions of UF processes. The properties of pollutants include the physical properties such as particle size and size distribution, diffusivity, solubility, and chemical properties such as polarity, hydrophilicity and interactions between contaminants and membrane surface. The membrane-related properties include the pore size, permeability, hydrophilicity and surface charge. The operating conditions include TMP, rejections, recoveries and feed water quality.

UF processes can be operated in two modes: 1) constant flux controlled by varing the driven pressure, and 2) constant pressure resulting in varying permeat flux. The constant pressure test was applied in this research. It is known that permeat flux is correlated to the transmembrane pressure in a certain range, in other words, permeat flux increases linearly with TMP within Darcy's law region (Xia, Li et al. 2004). The flux and TMP ranges examined in this study were within the Darcy's region. Permeat flux and TMP are important because membrane fouling can be controlled and the performance of membranes can be affected by ajusting these two parameters.

Pretreatment is often used to control membrane fouling. For hollow fiber membranes, contaminants can be backwashed with permeat water automatically, so the requirement of pretreatment is reduced (Kennedy, Kamanyi et al. 2008). Adequate pretreatment has a positive effect on controlling fouling. Guo et al. (2009) compared the performances of hollow fiber membrane systems with and without coagulation agents and found that the membrane system without coagulation agents could only remove particles larger than pore size, not the contaminants that led to membrane fouling over the time via clogging or cake layer formation. Moreover, when the colloidal microbial organisms adhered to the internal surfaces of membrane pore, irreversible fouling was established. While for the membrane system with coagulation agents, small particles aggregated, so it is easier for the hollow fiber to remove them. Pretreatment has a positive effect on UF, especially when large particles are contained in the source water, but is normally optional for UF processes.

To solve the fouling problem of UF membranes, backwash is commonly used, in which the water flow is reversed so the foulants adhered to the membrane as a cake layer can be washed away (Kennedy, Kamanyi et al. 2008). The required backwash frequencydepends on raw water quality. Cleaning is more easily adapted during intervals of the operation as used in the lab tests in this study.

Some membrane foulings can not cleaned by a simple physical method so chemical cleaning is needed. Chemical cleaning is often capable of recovering the performance to its initial status (Xia, Li et al. 2004, Chen, Mou et al. 2011). Xia et al. (2004) noticed that after the addition of 5% acid solution into the UF module, TMP was

decreased due to the removal of foulants sticking on the surface. The problem with the chemical cleaning includes its additional cost and the corrosive nature of some chemicals that may damage the membranes.

All methods discussed above for controlling the membrane fouling have advantages and disadvantages. As nanotechnology emerged leading to production of various nanomaterials, a new approach of developing anti-fouling membranes has been explored, in which nanomaterials are added into the membranes, and because of unique properties of varius nanomaterials, the membrane performance and anti-fouling characteristics could be improved.

1.3 Traditional commercial UF membranes

Most of the hollow fiber membranes are made of polymer materials, since fabrications of polymeric membranes are easy to achieve. Membranes are made of different polymers. For traditional commercial UF membranes, polymeric materials such as polysulfone (PS), polyether sulfone (PES), cellulose acetate (CA), polyvinylidenedifluoride (PVDF) and polyacrylonitrile (PAN) are most common used (Wagner 2001, Fane, Wang et al. 2011). The selection of membrane materials based on the operation conditions and application fields.

CA membrane dominated this industry in the first decades of membrane, but its thermal and chemical stabilities were low, making it difficult for operation under many conditions. It has narrow pH range for operation. PVDF and PS membranes are later

developed with a wider pH tolerance range, chemical and temperature stabilities, and become more commonly used.

Guo et al. (2009) used polyvinylchloride (PVC) to fabricate hollow fiber membrane. PVC was proven to have better resistance to chemical cleaning when compared with PS membranes. In another study, hollow fiber made of CA or PES but with the same configuration were compared (Nakatsuka, Nakate et al. 1996). The research demonstrated that CA membrane was more hydrophilic than PES membrane.

In summary, the performance of hollow fiber membranes highly depends on the material used for fabrication. The hydrophilicity is closely correlated to the type of polymer used and is important for the performance and antifouling properties of membrane, as the fouling tends to increase with decreasing hydrophilicity. Nevertheless, most traditional polymeric membranes subject to organic fouling, a critical issue that needs to be addressed for membrane application.

1.4 A critical issue of fouling for membrane application

Fouling of membranes leads to high energy requirements to maintain membrane performance, and hinders membrane applications for water treatment. "An increase in energy requirements and a reduction in throughput are a direct result of membrane fouling" (Holman and Ohlinger 2007).

Membrane fouling can result from the accumulation and/or deposition of rejected foulants from up stream on the membrane surface. Fouling occurs when the contaminants accumulate on a membrane surface, which contributes to irriversible

adhesion and can not be removed by cross-flow, backwash, and results in declining permeability (Escobar 2004). The effect of fouling on membrane can be expressed by decrease in flux and loss of permeability, since the flux is one of the most important factors controlling the economic feasibility of the membrane process (Vera 2000). A related parameter is permeability, which is obtained by normalizing flux against transmembrane pressure (TMP).

Membrane fouling can be caused by: a) pore narrowing, b) pore plugging, and 3) gel/cake formation (Tchobanoglous, Burton et al. 2003), which are illustrated in Fig. 1.

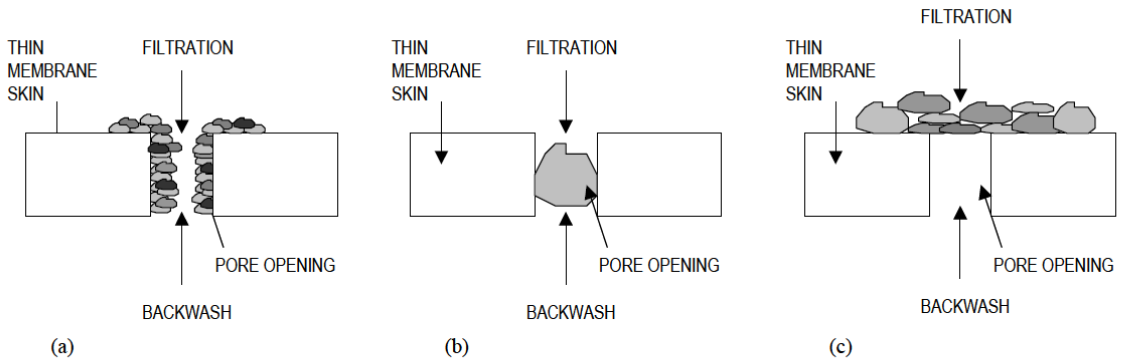

Fig. 1. Mechanisms for membrane fouling a) pore narrowing, b) pore plugging, and c) gel/cake formation (Bourgeous, Darby et al. 2001).

When the particles in feed stream are smaller or equal to the membrane pore size, pore narrowing and/or pore plugging will occur, leading to an increase of concentration polarization due to the adsorption of filtered particles within the pores (Holman and Ohlinger 2007). When the fouling layer became dense, irriversible membrane fouling could occur (Bessiere, Abidine et al. 2005), leading to pore blocking and gel/cake formation (Katsoufidou, Yiantsios et al. 2005). This type of fouling can always be

caused by inorganic particulate matter which is very likely to interact with membrane surface via chemical bonding.

Membrane fouling due to gel/cake formation is predominant in ultra filtration (UF) systems. This mode of fouling can result from biofilm formation (biological fouling) and organic fouling due to the natural organic matter (NOM). In addition, biofouling can be affected by fluid temperature, pH, nutrients, and flow conditions and etc. The mechanism of biofouling will be discussed in detail in section 1.3.

1.5 An introduction of transparent exopolymer particles (TEPs)

A critical challenge in membrane applicaion is to reduce organic and biological fouling. Bio-fouling is initiated by accumulation of organisms on membrane surfaces. With further growth of microorganisms, biofilm forms and results in membrane fouling that is difficult to clean. Typical organic fractions in natural water that have been detected by liquid chromatogram (organic carbon detection) are listed in Table. 1, including their size ranges and composition.

Table 2. Typical organic fractions in water and their sizes (Loreen O. Villacorte 2010).

Fractions	Size Range (Da)	Composition
Biopolymers	>20,000	Polysaccharides (e.g., TEPs) and protein
Humic substances	~1,000	Humic and fulvic acids
Building blocks	300-500	Weathering and oxidation products of humic
LMW organic acids	<350	All aliphatic low-molecular-weight organic acids

LMW neutrals	<350	Alcohols, aldehydes, ketones, and amino acids

With the deposition of organic substances on the membrane surface, microorganisms will colonize on the organic layer and cause biological fouling, since the organic substances provide nutrients to the colonized microorganisms. Additional deposition and accumulation of colloidal particles can be enhanced due to the sticky properties of the organisms (Villacorte, Kennedy et al. 2009).

In aquatic environments, extracellular polyssacharides can be generated from organisms (Hoagland, Rosowski et al. 1993). This organic substance is called extracellular polymeric substance (EPS), and TEP is considered as a subgroup of EPS in aquatic environments (Berman 2007). While compared to EPS which exists as cell coatings or dissolved slimes, TEP exists as individual particles (Alldredge, Passow et al. 1993). This difference contributes to the aggregation of individual TEP particles. While TEP has been overlooked for many years due to their invisibility, it has believed that TEPs are ubiquitous in most aquatic environments, and they play an important role in biofilm formation and membrane fouling.

TEPs are mainly made up of acidic and surface active polyssacharide (Mopper, Schultz et al. 1992), such as fucose and rahmnose (Mopper, zhou et al. 1995), These materials are hydrophilic, and have a C:N ratio always higher than the normal Redfield ratio of common organisms (Redfield, Ketchum et al. 1963). TEPs are highly surface active due to their high fraction of sulfate halfester groups and can form hydrogen bonds and/or metal ion bridges (Mopper, zhou et al. 1995). TEPs can be identified and

measured by alcian blue staining, but the accurate chemical composition of TEP is highly variable and still remains unknown, since their chemical structure and composition rely on where they are coming from (Passow 2002). TEPs can be generated abiotically from dissolved organic exudation products via coagulation and gelation processes (Passow 2000). They can also be released from gelatinous matter surrounding diatoms and algea, and generated at senescence of algea (Hans-Peter Grossart 1997). In this research, chlorella vulgaris was caltivated for generating TEP. The TEP particles can aggregate further to form marine or lake snow as a result of abundance of colloidal particles. This phenomenon has been illustrated in Fig. 2, where, a) shows the newly prepared water sample with TEPs and small amount of alcian blue dye, which is clear and transparent, and b) is the same solution that had been aged for 1 week.

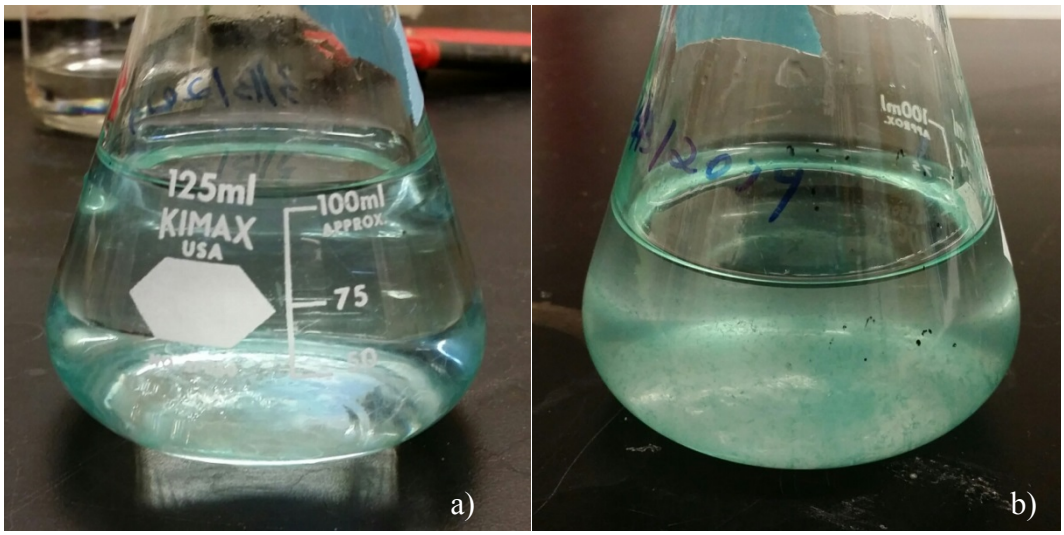

Fig. 2. An illustration of TEP aggregation to form lake snow. a) the fresh water sample with TEP and small amount of alcian blue, b) the same solution after aging for 1 week.

The physical properties of TEPs are highly relevant to the biofilm formation and membrane fouling. TEPs are gel-like and can appear in many forms, such as, amorphous blobs, filaments, sheets and clouds, with their size ranging from colloidal (1kDa) to 100s of microns (Passow 2002). TEPs are capable of passing through filter pores smaller than their sizes due to their gel-like properties and high flexibility in size and shape (Passow and Alldredge 1995). The particle size distribution was also analyzed in this study, and the result showed that TEPs of large size dominated the size distribution due to the aggregation of colloidal particles in consistence with the literature report (Engel 1998). In addition, TEPs are very sticky and negatively charged, and sometimes colonized by bateria (Berman 2007). It has been reported, that stickness of TEPs can reach 2 to 4 orders of magnitude larger than phytoplankton, which means TEP plays an important role in increasing the stickness of natural substances (Engel 2000).

Based on size, TEPs can be classified into colloidal (c-TEP, 0.05 to 0.4 μm) and particulate (p-TEP, >0.4 μm) forms, with the colloidal TEP four times more abundant than particulate TEP (Villacorte, Kennedy et al. 2009). C-TEP plays an important role in biofilm formationa and membrane fouling, and can not be easily removed from water due to their small size and gel-like properties.

1.6 Biofilm formation and TEP Fouling Mechanism

A critical issue in water treatment industry is to control and minimize biofilm formation and accumulation (Kumar M 2006). The biofilm formed on membrane surfaces leads to membrane fouling which will reduce the efficiency of filtration by increasing trans-membrane pressure (TMP) and hydaulic resistance, subsquently decrease the permeability.

TEP is the main initiator of biofilm because of its sticky nature and conductive to bacterial colonization. It is mainly made up of polysaccharides that can serve as nutritional sources for bacteria. The process of biofilm build up initiated by TEP in flowing water is illustrated in Fig. 3.

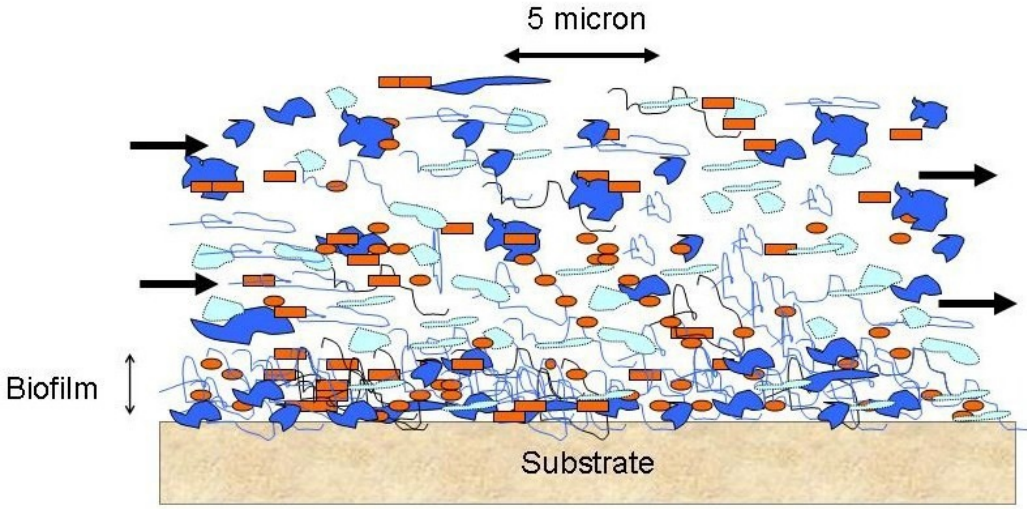

Fig. 3. Mechanism of biofilm formation on substrate surface in flowing water (Berman and Holenberg 2005).

It is proposed that once TEPs (dark blue), with some of them colonized by bacteria (red) adhere to the substrate surface due to their sticky property, they provide a nutritional environment for further growth of other microorganisms and bacteria. The nutrition provided by TEPs can be easily absorbed by the colonized baterica. Subsquently, other colloidal material (light blue) including some decomposed organisms containing amino acids and additional TEPs will adhere to the surface, providing further nutrition for microbial growth. The whole process helps to eventually establish the biofilm.

The mechanisms of membrane fouling caused by TEP can be illustrated by combining biofilm formation theory with membrane fouling mechanisms in chapter 1.1. Once the biofilm is established and buildup on the membrane surface, gel/cake formation occurs, which plugs the pore of membrane and the channels inside the solid contaminant particles, as illustrated in Fig. 4.

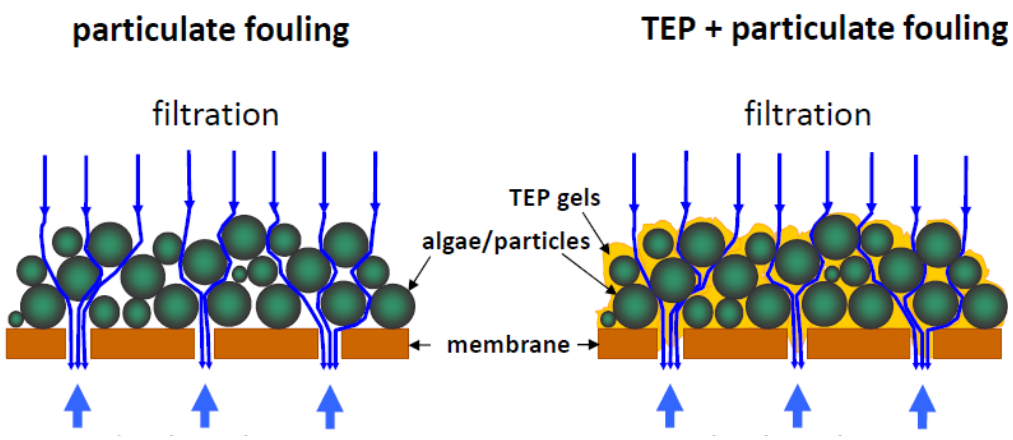

Fig. 4. Schematic diagram of TEP fouling (J.C. Schippers 2008).

As more and more gel-like TEPs adhere to the surface and aggregate, the hydraulic resistance and TMP will increase, resulting in the reduction of the membrane permeability. Simple physical backwashing is not capable of removing such sticky contaminants, hence, irriversible fouling occurs. The polysaccharides in TEP may also contribute to the membrane fouling by forming hydrogen bonds with other colloidal particles.

1.7 An overview of microalgea: *Chlorella vulgaris*

Most of the TEP precursors are produced by microalgea in the natural environments (Engel and Passow 2001, Passow 2001). Surprisingly, the influence of TEPs on the filtration of microalgea, which is cultivated for commercial applications has not been reported up to now. Microalgea are photosynthetic organisms with a great potential of being cultivated as energy crops (Discart, Bilad et al. 2013). Membrane techniques are most commonly applied in harvesting microalgea due to its high retention of biomass and low energy requirement (Bilad, Vandamme et al. 2012, Lee, Liao et al.

2012), therefore, understanding the fouling of membranes by algea and their exudations and developing approaches to mitigate the impact of such fouling are important to maintain high efficiency of the algal culture process.

Microalgea are abundant and diverse in most aquatic environment, and during algal bloom, the extracellular substance is released which has a negative effect on drinking water treatment. The release rates of these compounds depend on the algal species and environmental conditions. One of the main objectives of this study is to investigate the properties of TEPs obtained from *Chlorella Vulgaris* broth solution. *Chlorella vulgaris* is a well characterized species of microalgea that is involved in unfavorable algal blooms (Jacquet, Briand et al. 2005), on the other hand, it has an excellent potential to be used for large-scale commercial CO_2 capture and lipid production (Mallick, Mandal et al. 2012). In this study, different fractions including soluble microbial particles, extra polymeric substance were separated from the broth solution to obtain most of the TEPs for further study.

1.8 N-TiO_2 nanoparticles modified hollow fiber membrane

In order to reduce organic fouling and extend the lifetime of membrane, many attemps have been made tomodify UF membrane. Ahmad (2011) had applied SiO_2 modified PSF functional membrane in oil-in-water separation, and due to the excellent properties of SiO_2, the antifouling property of UF membrane was improved.

Zhang, Q et al. (2014) examined the use of carbon nanotube (CNT) to make conductive UF membrane. When the membrane system was connected to an external

DC power, the negatively charged organic foulants were excluded, leading to less organic fouling. In general, modifications that enhance membrane surface hydrophilicity improve their fouling resistance.

Here we suppose to modify PVDF hollow fiber membrane by adding TiO2 nanoparticles into the matrix. TiO_2 nanoparticles have unique photo catalytic properties and chemical and temperature stability (Mills and Le Hunte 1997, Paz 2010). One disadvantage with normal TiO_2 particles is its wide activation band gap of 3.2 eV, indicating that it can only be activated by UV light (Chen and Mao 2007). Its commercial application will incur significant energy cost. To increase the efficiency of membrane processes, many attempts have been paid to synthesis TiO_2 that can be activated by visible light, such as by doping noble metal (Sangpour, Hashemi et al. 2010) and other constituents, and non-metal doping (Xu, Gao et al. 2002). Nitrogen doped titanium dioxide (N-TiO2) was found to be efficient in photo catalytic activity with visible light exposure, because the energy band gap is narrowed with N doping. This may be due to the interaction between 2p states of N and O elements, the energy of which are close to each other.

With the help of photo degradation of contaminants, membrane fouling is reduced. The mechanism of how TiO2 contributes to the antifouling properties of membrane is illustrated in Fig. 5.

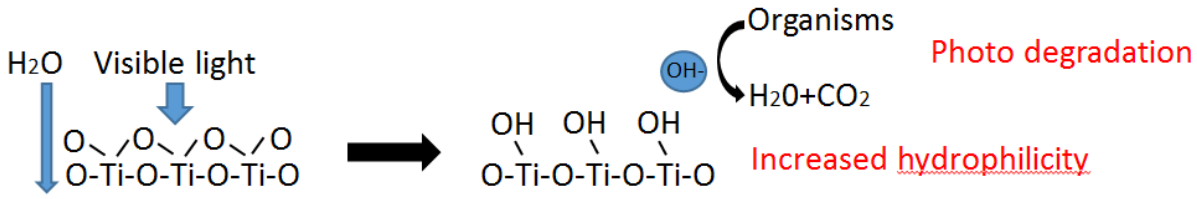

Fig. 5. Mechanism of photo catalytic TiO_2 activated by visible light irradiation and its contributions to organic fouling reduction.

As the N-TiO_2 on the membrane is exposed to visible light and in contact with water, the nanoparticles are activated and interacts with the water to form a hydroxy radicals on the TiO_2 surface. This may change the membrane surface property and increase the membrane hydrophilicity. Additionally the oxidative hydroxy will contributes to the photo degradation of organic chemicals and thus prevent formation of cake/gel layer and membrane fouling.

In this study, we have a) synthesized N-TiO_2 nanoparticles, b) fabricated PVDF/N-TiO_2 hollow fiber membrane via the spinning method and c) evaluated the performance of the membrane under the influence of TEPs. The experimental procedure and results will be discussed in the following sections.

CHAPTER 2. METHODOLOGY

2.1 Materials

Alcian Blue 8GX (Sigma Aldrich) was used as stain ofr observing and measuring TEP. In synthesis of nitrogen doped titanium dioxide nanoparticles (N-TiO_2 NPs), ammonia aqueous solution (28-30%, Sigma-Aldrich) was selected as nitrogen source and tetrabutyl titanate ($Ti(OBu)_4$, 97%, Sigma-Aldrich) was used as precursor. Titania (Degussa P25, Degussa Corporation, Germany) was used as a reference for comparison. During the fabrication of modified PVDF hollow fiber membranes, poly(vinylidene fluoride) (PVDF) with an average molecular weight (MW) of 180 kDa was obtained from Sigma-Aldrich and dried for 3 h at 120 °C before usage. Polyvinylpyrrolidone (PVP, Sigma-Aldrich) with average MW of 10 kDa was chosen as porogen, and N, N-Dimethylacetamide (DMAc, 99.5%, Sigma-Aldrich) was selected as solvent. Deionized (DI) water produced by Millipore DI system (Synergy 185,18.2 MΩ·cm) was used for solution preparation and most water involved in experiments. All other chemicals were purchased from Sigma-Aldrich.

2.2 Growth of *Chlorella Vulgaris*

Chlorella vulgaris broth was cultured to produce TEPs, as the literature has shown that TEP could be successfully separated from *chlorella vulgaris* broth (Discart, Bilad et al. 2013) . *Chlorella vulgaris* was cultivated in a 7.5×7.5×12.5 inch cuboid transparent glass container, and the algea was kept exposed to a sunlight lamp 24h/day for photosynthesis and growth. The algea cells could aggregate and adhere to the wall

surfaces of the container, so to solve this problem and keep an uniform distribution of algea, the broth was stirred at 350rpm 24h/day using stirrer (Fisher Scientific). The *chlorella vulgaris* was fed once a week with certain nutrition (0.1% v/v) listed in table 3.

Table 3. Components of nutrient solution for chlorella vulgaris.

$NaNO_3$ 62.2g/L	NaCl 25.1g/L	$FeCl_3$ 3.72g/L	SO_4^{-2}
$NaHCO_3$ 84g/L	$FeCl_2 \cdot 4H_2O$ 2g/L	EDTA 4.2g/L	
K_2HPO_4 75g/L			

2.3 Separation of TEP from algal culture broth

TEP was generated during the algal growth. To minimize the interference of other components in the broth, fractions were separated using an established method of Discart (2013) as shown schematically in Fig. 6.

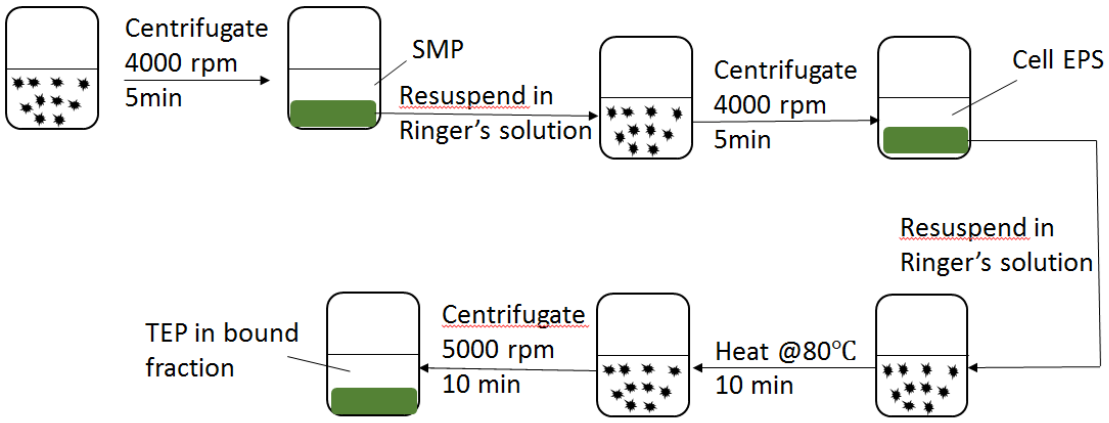

Fig. 6. Schematic diagram of TEP separation from algal culture broth.

Firstly the soluble fraction was obtained as the supernatant after centrifugation (Centrifuge 5810 R, eppendorf Corporation) at 5000 rpm for 5 min. Some of the c-TEP

was in this fraction. The $Cell^{EPS}$ fraction was obtained by resuspending the cell pellet from the first step in Ringer's solution (see Table 4 for composition), then this fraction was obtained as the supernatant after centrifugation at 5000rpm for 5 min again.

Table 4. Fractions of Ringer's solution.

Components	$CaCl_2$	KCl	$NaHCO_3$	NaCl
Amount	0.12 g/L	0.105 g/L	0.05 g/L	2.25 g/L

To get the TEPs in bound fraction, the obtained pellet was resuspended again in Ringer's solution and heated at 80 °C for 10 min, and subsquently the hot solution was centrifuged at 6000 rpm for 10 min, so the bound fraction was extracted as the supernatant. The final solution of TEP was obtained by mixing all the supernatants.

The TEP solution was stored in refrigerator at 4 °C, and measured and used within 1 week.

2.4 Properties of TEP

The properties of TEP solution was analyzed for its size distribution and zeta potential (Zetasizer, Nano-ZS, Malvern Corporation). The suspension was measured twice to give an average particle size.

2.5 Observation and measurement of TEPs

The observation and measurement of TEP were based on Alcian Blue staining method. TEPs could be visible after stained by Alcian Blue stain solution. The stock

solution was obtained by adding 0.03 g Alcian Blue 8 GX powder to 30ml 3% acetic acid and resulting in an 1% stock solution. The stock solution was stored at 4 ℃ and avoid light exposure prior to use. Before usage the stock solution was diluted 1:30 to a 0.03% Alcian Blue stain solution (Logan, Grossart et al. 1994). Furthermore, in order to avoid the effect of remaining Alican Blue on the filter, the solution was pre-filtered before usage.

In this study, 0.1 μm polycarbonate filter (Isopore^{TM}, Millipore Corporation) was selected for TEP observation and measurement. Previous studies showed that the size of TEP ranges from 0.1 μm to 200 μm, so polycarbonate mebrane with a diameter of 0.1 μm is capable of retaining most TEPs. Before the observation of TEPs, a slide would be prepared. Firstly, 10 ml of TEP water sample was filtered through the 0.1μm polycarbonate filter paper placed on a 25mm filter holder (GelmanSciences) using vaccum filtration (VP50, LabTech) at 0.2 psi. Then 0.5ml of the 0.03% alcian blue solution was added to the filter paper, After reaction of alcian blue with TEPs takes for 15s, the suspension was vaccum filtered by the membrane. Followed by washing with DI water to remove the excess dye. A slide was made by simply placing the filter with Alcian Blue bounded TEP on a glass slide covered by a glass slide. The sample was then examined by a microscope (AXIO Scope. A1, ZEISS Corporation) and immaged by a digital camera (AxioCam, ZEISS) connected to the computer.

To get the rejection of TEP through the membrane, TEP concentration was detected in a similar way using Alcian Blue staining method. The measurement of TEP

was based on a linear relationship betwwen the quantity of TEP and the amount of stain binding to it (Ramus 1977).

First, 0.02% Alcian Blue stain was prepared using acetate buffer at pH of 2.5, and the stain was also pre-filtered through the 0.1μm polycarbonate filter. Then 5ml of TEP solution was vaccum filtered through the 0.1μm polycarbonate filter at 0.2 psi. An 0.5 ml of 0.02% Alcian Blue solution was added to the filter paper and reacted for 30s, then the filter paper was washed by filtering 1 ml of DI water to remove the excess stain. Finally the filter paper was transferred to a 50 ml beaker and soaked in 6 ml of 80% H_2SO_4 for 2 hr. The alcian blue binded to TEPs was eluted from the filter to the H_2SO_4 solution, which was analyzed by using spectrophotometer (CARY 50, varian Coporation) at 787 nm wavelength.

The same procedure was performed with DI water as reference, where the average absorbance of eluted stain from blank filter was measured for calibration to avoid the effect of absorption. Here relative values represented by absorbance was used instead of absolute concentration. The absorbance was propotional to the concentration of TEP, implying that the absolute concentration of TEP can be calculated by mutiplying a parameter by the absorbance. So the concentration of TEP was represented in the unit of absorbance per liter of TEP solution filtered [abs/cm/L of TEP]. Finally the concentration of TEP solution can be calculated using Eq. 1.

$$C_{TEP} = (A_{787} - B_{787}) * 1000/V_{TEP} \qquad (1)$$

Where A_{787} and B_{787} were the absorbances of stain eluted from TEP and blank filter, and V_{TEP} was the volume of TEP solution filtered.

2.6 Synthesis of N-TiO_2 NPs

A method revised from Wang, Cai et al. (2005) was adopted here to synthesis N-TiO_2 NPs. The procedure was carried out by adding dropwisely 10 ml of ammonia solution into 20 ml of $Ti(OBu)_4$ solution and let the hydrolysis reaction occur for 10 min under stirring at room temperature. The precursor was then dried in an oven at 120 ℃ for 2 h. N-TiO_2 NPs were finally obtained by calcinating the precursor at 400 ℃ for 1 h until the color of the powder switched from white to brown.

2.7 Fabrications of hollow fiber membranes

The N-TiO_2 modified PVDF mixed matrix hollow fiber membranes were fabricated on a custom-designed single-head spinning machine by phase inversion method based on the previous work of Jun Yin (2013).

The dope solution was obtained by dispersing 1% of N-TiO_2 NPs into 75% DMAc solvent and sonicated for about 1 h to get an uniform distribution. Subsquently, 4% of PVP was added to the mixture and stirred for 30min. Finally the spinning polymer solution was obtained by adding 20% of PVDF and stirring at 40~50℃ for 6~8 h. The dope solution was kept overnight for degassing prior to usage. The spinning system and the fabrication processes were shown schematically in Fig. 7.

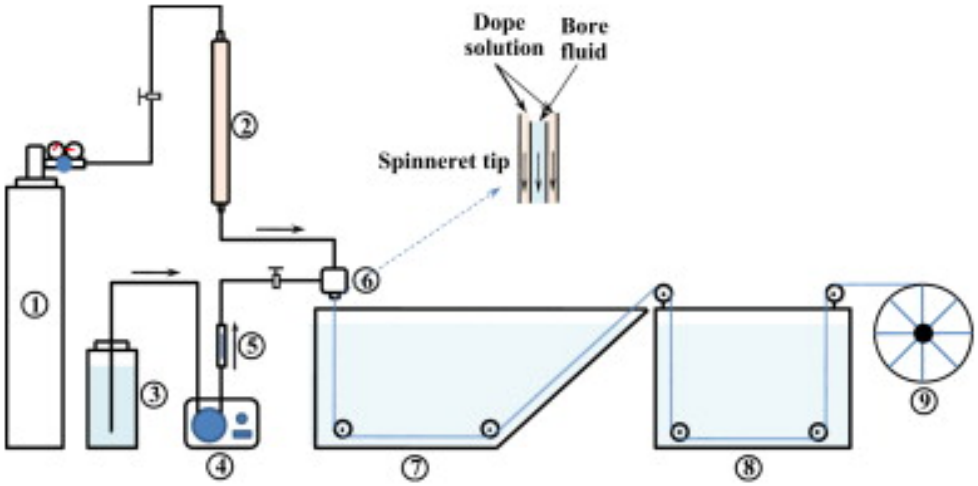

Fig. 7. Schematic diagram of the custom-designed single-head spinning system: (1) high purity nitrogen, (2) dope solution, (3) bore fluid, (4) gear pump, (5) flow meter, (6) spinneret, (7) coagulation bath, (8) washing bath, (9) collecting drum (Yin, Zhu et al. 2013).

The polymer solution was pressed into the spinneret by high purity nitrogen under certain pressure. DI water was selected as bore fluid, and was pumped into the inner tube of spinneret. Hollow fibers were produced through the phase inversion in the coagulation bath when the dope solution and bore fluid met each other at the bottom of the spineret. The produced hollow fibers were pre-washed in wash bath and collected by the collecting drum, and was rinsed with DI water for at least 24 h to remove the remaining solvent prior to use. Some of the experimental parameters were listed in Table 5.

Table 5. Experimental parameters of hollow fiber fabrication.

Parameter	Condition
Spinneret OD/ID	1.0 mm/0.6 mm
Spinning temperature (℃)	25
Dope solution	PVDF/PVP/DMAc
Concentration (wt. %)	20/4/75
Bore fluid composition	DI water
Bore fluid flowrate (ml/min)	0.6
Coagulant and washing bath	Tap water

In this study, three types of hollow fiber membranes were made for comparison: original PVDF membrane, represented by PVDF, commercial P25 TiO_2 NPs modified PVDF membrane, named PVDF/P25, and PVDF/N-TiO_2 mixed matrix membrane. Here the PVDF and PVDF/P25 membranes served as references.

2.8 Membrane characterization and performance assessment

Characterization of membrane was carrired out by scanning electron microscopy (SEM) on Quanta FEG 600. Preparation of membrane sample for SEM was performed simply by drying a segment of hollow fiber at room temperature. Prior to SEM imaging, these specimens were coated by platinum at 20 mA for 60s.

Hydrophilicity of the membrane was evaluated by measuring the contact angle of pure water on the membrane surface according to the sessile drop method. The specimens were made by drying some pieces of membrnae and closely aligning them on a flat tape, then flattening. A video contact angle system (VCA-2500 XE, AST products,

Billerica, MA) was employed to carry out the analysis. To minimize the error, at least 8 measurements of stablized contact angles at different sites of the samples were obtained to calculate the average value.

To evaluate the membrane performance such as the pure water flux, permeate flux, rejection of solute and fouling resistance, a low pressure cross-flow UF system was employed according to the previous work by Jun Yin (Yin, Zhu et al. 2013). A piece of hollow fiber membrane was located in a quartz tube module for later operation and the tube was sealed with epoxy resin. The effective area of the membrane was around 0.0011 m^2. A schematic diagram of the filtration system was illustrated in Fig. 8.

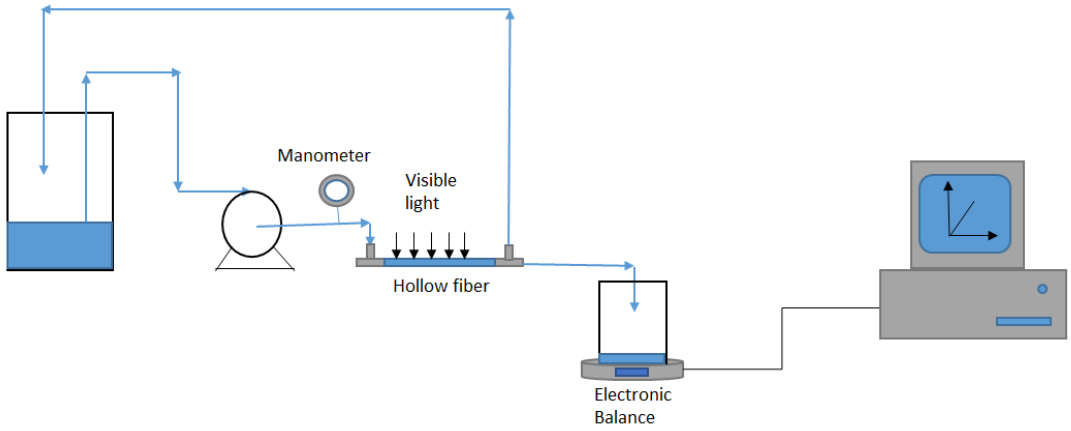

Fig. 8. Schematic diagram of the filtration system.

Prior to test, DI water was pumped into the system under a constant TMP of 8 psi for 3 h until a steady state was reached. Pure water flux was measured first. This was achieved by collecting and weighing the permeate water with an electronic balance as a function of time was controlled and recorded by the LabVIEW system (National Instruments LabVIEW 8.2 with Ohaus digital balance). Fluxes of pure water were

obtained under different driven forces, a curve of flux versus pressure can be produced due to the proportional relationship. Right after the pure water flux test, the previously mentioned TEP solution was employed as the feed solution, and filtration performance wa assessed in a similar way. The permeate flux can be calculated using Eq. 2.

$$J = \frac{V_p}{A \cdot t} \tag{2}$$

Where J is the flux (L/m^2/h), V_p represents the permeat volume (L), A refers to membrane area (m^2), and t is the duration of filtration (h).

Visible light irradiation (F32T8 FLUORESCENT LIGHTS, 10.9 Mw/cm^2, Philips) was employed and maintained all the way until the end of the measurement, and flux measurements without visible light were also carried out as a reference. Same procedures were performed on PVDF/N-TiO_2, PVDF/P25 and PVDF blank membranes for comparison.

The concentration of original TEP solution was measured according to the method discussed in section 2.4, and the result was used for calculating the normalized flux by dividing the flux by concentration. Furthermore, the permeate solutions and concentrated solutions were collected at the same time and measured using the Alcian Blue staining method. The rejection of solute was calculated by Eq. 3.

$$R = \left(1 - \frac{C_p}{C_f}\right) \times 100\% \tag{3}$$

Where R is the rejection ratio, C_p and C_f represent the TEP concentrations of permeat and feed solution, respectively.

CHAPTER 3. RESULTS AND DISCUSSION

3.1 TEP monitoring

The images of TEP obtained from microscopy using alcian blue staining method are shown in Fig. 9. TEPs can be found as the colloidal aggregations in blue color. The result was consistent with that observed by Lorren Q. Villacorte et al. (2010). TEP aggregates can be found around the algal cells (green cells), since during the separation of TEP from the *chlorella vulgarise* broth, some of the algal cells were destroyed and the polysaccharide inside the cells was released. TEPs were observed in colloidal and particulate configurations, and the size of TEP aggregations was estimated in the image as around 80 μm, which was within the size range obtained by Passow (2001).

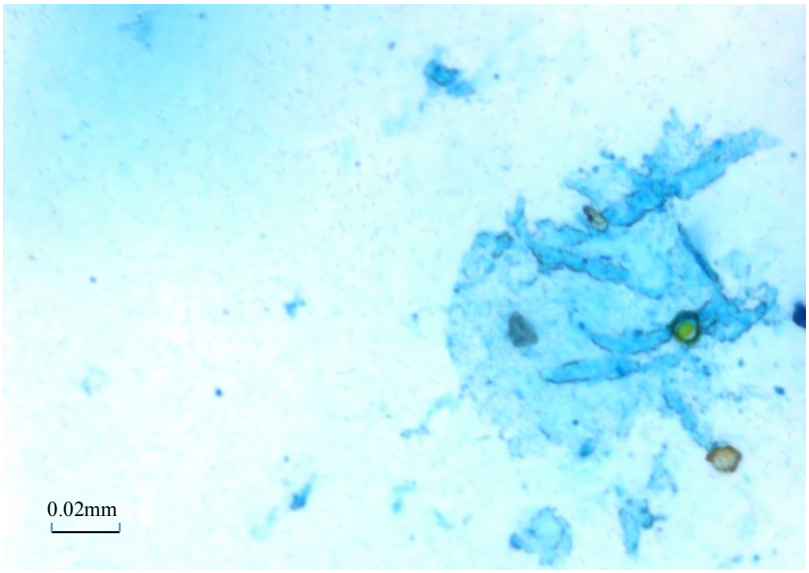

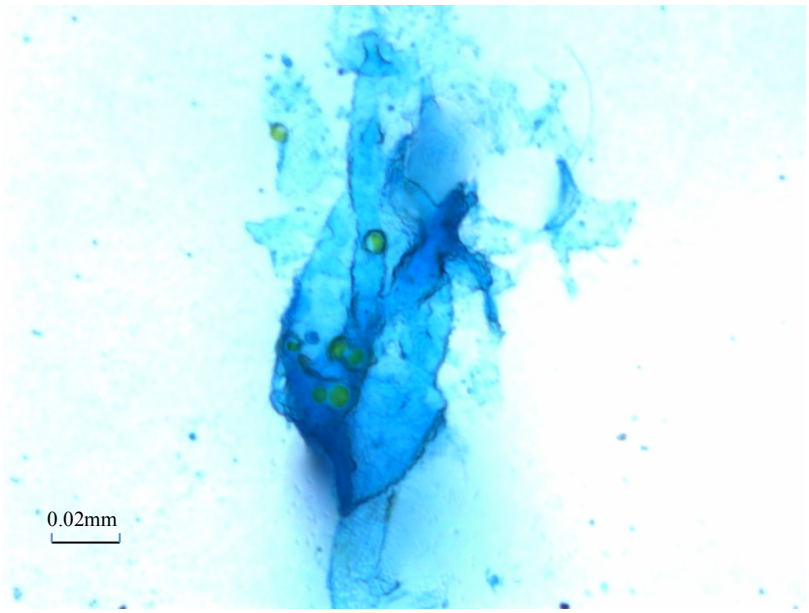

Fig. 9. Optical microscope photographs of TEPs after staining with Alcian Blue.

3.2 Size distribution and zeta potential of TEP

The size distribution of TEP solution was obtained using the zeta sizer apparatus. It is illustrated in Fig. 10 that according to the two measurements, two peaks can be seen representing that there are two groups of TEP, namely, c-TEP which was the small peak and p-TEP which referred to the big peak. The average particle size of TEPs was obtained as 2.57 μm, which was within the size range mentioned in earlier section. The actual average size of particles are likely smaller than the measured one due to the water shell adhering to the particles in the solution.

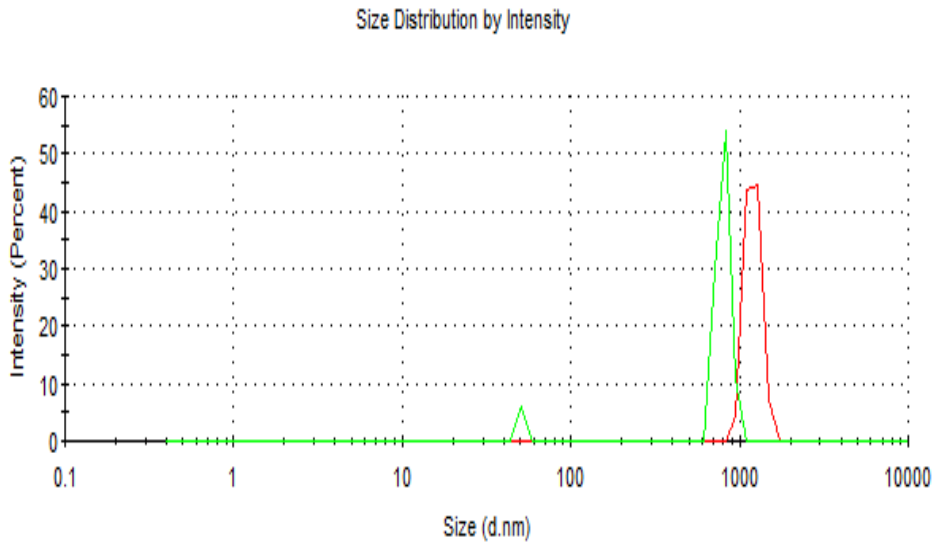

Fig. 10. Size distribution of TEP.

The average pH values of the TEP solutions used for flux test was at 7.8, at which pH, the corresponding zeta potential was approximately -13.3 mV. Therefore, the TEPs in the solution used for the flux test was negatively charged, which was consistent with the conditions used by Discart (2013). Ghosh and Bandyopadhyay examined why polysaccharides were negatively charged (2012). It appeared that as the main fraction of TEPs, polysaccharides were deprotonated at a pH range higher than its pKa (see in Fig. 11). The pH of the water used in the flux test was at 7.8, which is higher than the pK_a of polysaccharides, so deprotonation of –COOH occurs, rendering the negatively charged TEPs.

pH << pKa	**pH = pKa**	**pH >> pKa**
$R\text{-}CH_2\text{-}COOH$	$R\text{-}CH_2\text{-}COOH$	$R\text{-}CH_2\text{-}COOH$
~~ COOH	~~~~ COO^-/~~~ COOH	~~~~~ COO^-

Fig. 11. Variation of charge density on the polyssacharides at various pH values.

3.3 Characterization of PVDF/N-TiO_2 membrane

The outside surface images of the three types of membranes are shown in Fig. 11. In a1), b1) and c1), it is found that all membranes are dense and tight. When the images were magnified to a larger scale, N-TiO_2 nanoparticles (white points) become visible in c2) as uniformly dispersed dots on the membrane surface. The pore size of original PVDF hollow fiber membrane was estimated to be about 50 nm. The pore sizes of PVDF/P25 and PVDF/N-TiO_2 with added nanoparticles higher, which could account for the difference of rejection between original PVDF membrane and other two membranes discussed later. In Fig. 11 (b3), P25 TiO_2 nanoparticles can be seen as aggregates with less uniformed dispersion.

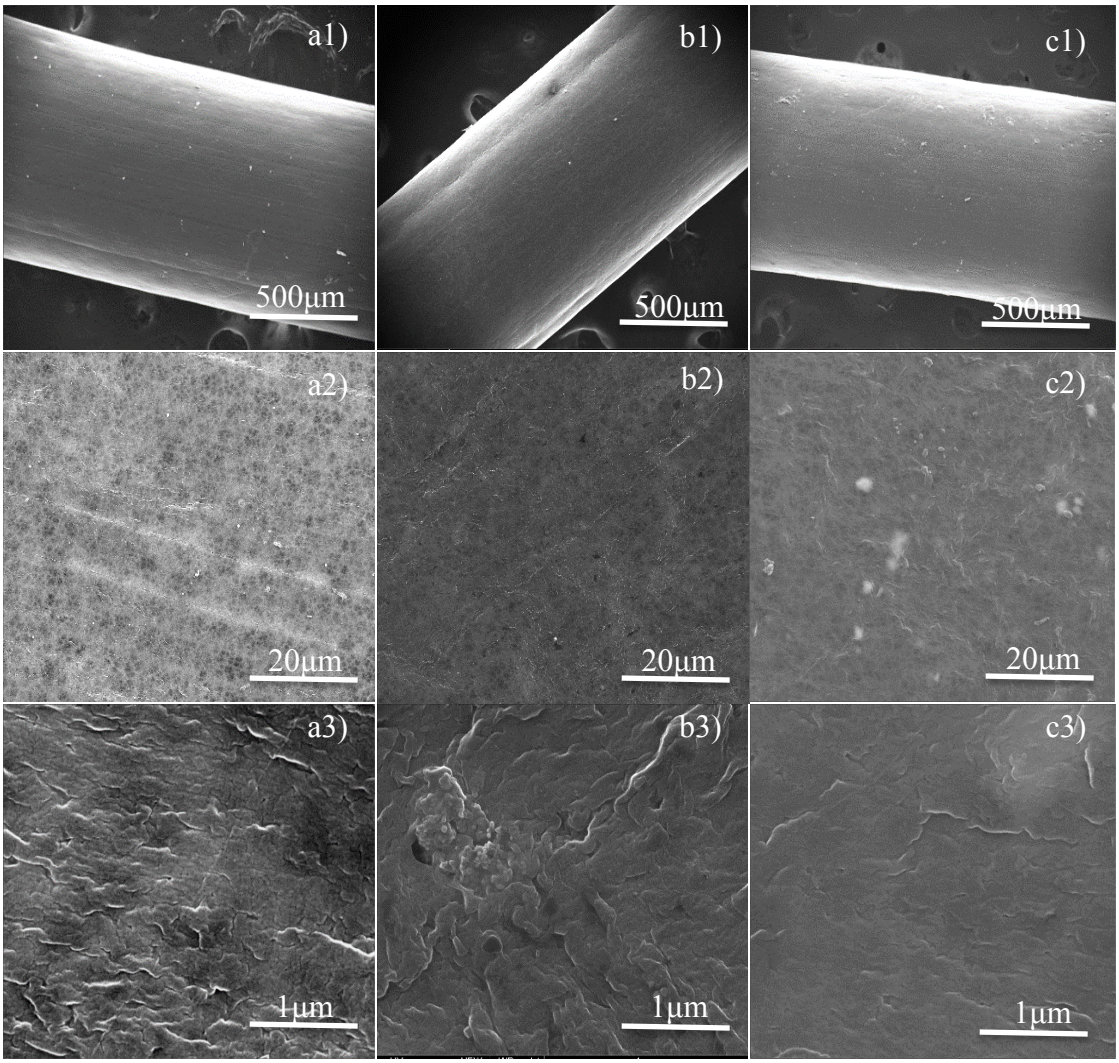

Fig. 12. SEM photographs of a1) original PVDF, ×150, b1) PVDF/P25, ×150, c1) PVDF/N-TiO_2, ×150, a2) original PVDF, ×5k, b2) PVDF/P25, ×5k, c2) PVDF/N-TiO_2, ×5k, a3) original PVDF, ×75k, b3) PVDF/P25, ×75k, c3) PVDF/N-TiO_2, ×75k.

3.4 Hollow fiber membrane performance

Dark and visible light irradiation conditions were applied to evaluate the membrane fouling behaviors with TEP solutions serving as model foulant. Rejcetions of TEP through PVDF, PVDF/P25 and PVDF/N-TiO_2 hollow fiber membranes were measured and listed in table 6.

Table 6. Rejections of three types of hollow fiber membrane under different irradiation conditions.

Membranes	PVDF	PVDF visible light irradiation	PVDF/P25	PVDF/P25 visible light irradiation	PVDF/N-TiO_2	PVDF/N-TiO_2 visible light irradiation
Rejection	97.30%	99.97%	90.60%	86.45%	85.56%	86.86%

The results shown in Table 6 implies that all the hollow fiber membranes have high rejections of TEPs more than 85% no matter with or without visible light irradiation. Furthermore, the rejection of PVDF/P25 and PVDF/N-TiO_2 were repectively 7% and 10% lower than the original PVDF membranes. The reason for this phenomenon was likely that with the addition of nanoparticles, the surface morphology of membranes were changed.

Pure water flux as a function of TMP are illustrated in Fig. 14. According to the curves, the pure water flux of original PVDF membrane at 8 psi under visible light irradiation and dark conditions were 23.03±0.81 L/m^2/hand 23.83±0.41 L/m^2/h repectively. With the addition of TiO_2 nanoparticles, the pure water flux under the same condition was increased due to the high hydrophlicity of TiO_2. Little difference was observed between the pure water flux of PVDF/P25 under dark condition and visible light irradiation condition, suggesting that P25 can not be activated efficiently by visible light irradiation. The pure water fluxes of PVDF/P25 at 8 psi were at 25.44±0.61 L/m^2/h and 25.34±1.06 L/m^2/h under visible light and dark conditions. The PVDF/N-TiO_2 membrane showed a higher hydrophilicity and also a higher pure water flux. The

PVDF/N-TiO_2 membrane with visible light irradiation had the highest pure water flux among all other membranes. It is proposed that the N-TiO_2 nanoparticles were activated by visible light due to the nitrogen doping, resulting in the highest flux.

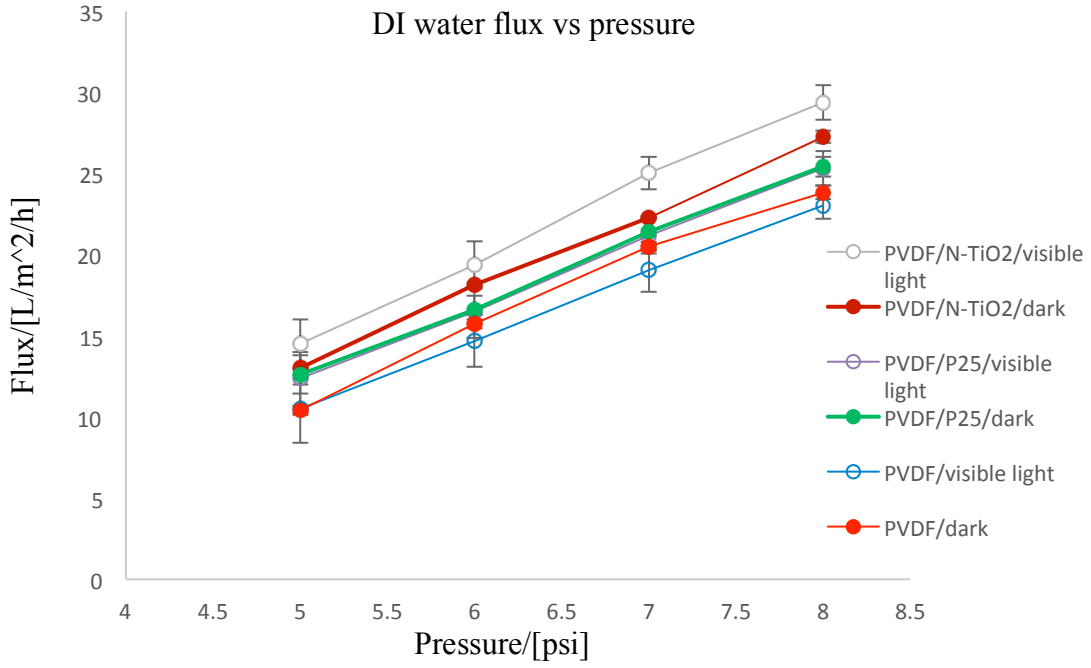

Fig. 13. Pure water flux vs. pressure.

The results of pure water flux of membranes were consistent with hydrophlicities obtained by contact angle measurements shown in Fig. 15(a-c). The average water contact angles of PVDF, PVDF/P25 and PVDF/N-TiO2 hollow fiber membranes were obtained as 54.62° , 49.27° and 42.33° , which means that the PVDF/N-TiO_2 membrane has the highest surface hydrophilicity.

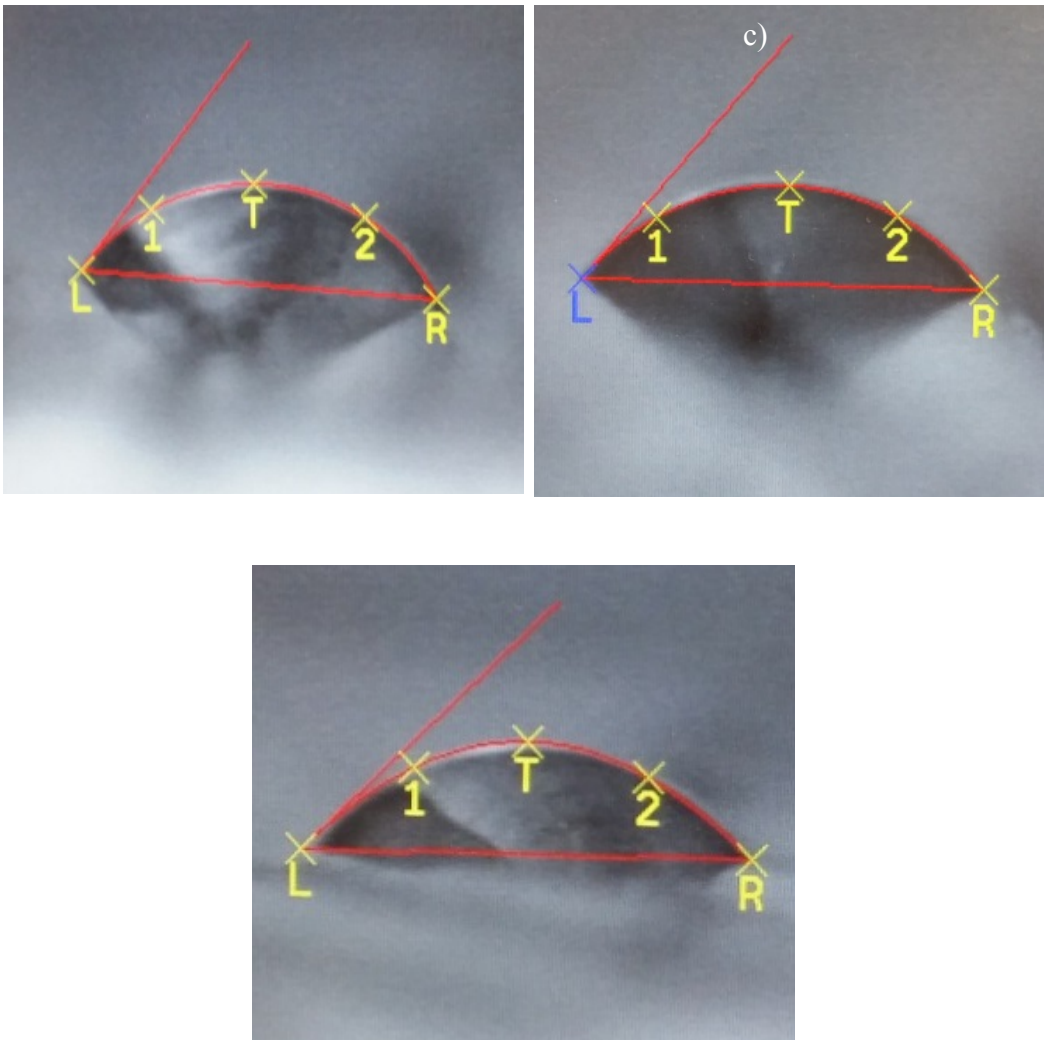

Fig. 14. Contact angles of hollow fiber membranes, a) PVDF, b) PVDF/P25, c) PVDF/N-TiO_2.

Evaluations of membrane performance were carried out under various irradiation conditions by using TEP as a model foulant. The fouling resistances of the HFMs were evaluated by comaparing water flux and flux decrease together. The water flux decrease is shown in Table. 7.

Table 7. Flux decreases of HFMs under dark and visible light irradiation conditions.

HFMs	PVDF/ Dark	PVDF/Visible light	PVDF/P25/ Dark	PVDF/P25/ Visible light	PVDF/N-TiO_2/Dark	PVDF/N-TiO_2/Visible light
Flux Decrease	28.5%	34.3%	30.1%	30.3%	32.9%	46.7%

The water fluxes are shown in Fig. 15. With TEPs, the water flux through the original PVDF membranes are represented by two curves near the bottom in the figure, i.e., their fluxes are lower than those through the mixed matrix membranes. This is consistent with the facts that there is no hydrophilicity enhancement or photo catalytic activities with the original PVDF.

PVDF/P25 membrane showed much better antifouling properties than that of the original PVDF membrane. Furthermore, the fouling resistance of PVDF/P25 membrane was similar to that of PVDF/N-TiO_2 membrane under the dark condition. Both PVDF/P25 and PVDF/N-TiO_2 membrane had better fouling resistance and higher water flux than the original PVDF membrane under dark condition, indicating the attribution of TiO_2 nanoparticles to enhanced hydrophilicity of the membrane and water flux. Under the visible light irradiation, the water flux with the PVDF/N-TiO_2 is higher than that of PVDF/P25, demonstrating that the activation of PVDF/N-TiO_2 under visible light has provided additional hydrophilicity for faster water filtration. The adsorption of organic chemicals on membrane was reduced with the enhanced surface hydrophilicity, so the foulants adhered to the membrane surface could then be easily removed by cross flow.

Two cycles of flux tests were carried out by washing the system twice during the interval and after the second flux test of TEP solution. The water fluxes of all membranes during the second cycle were lower than that of the first cycle, and the same phenomenon was observed for the two DI water washing processes. Both of these flux decreases were caused by irriversible fouling which could not be removed simply by physical washing.

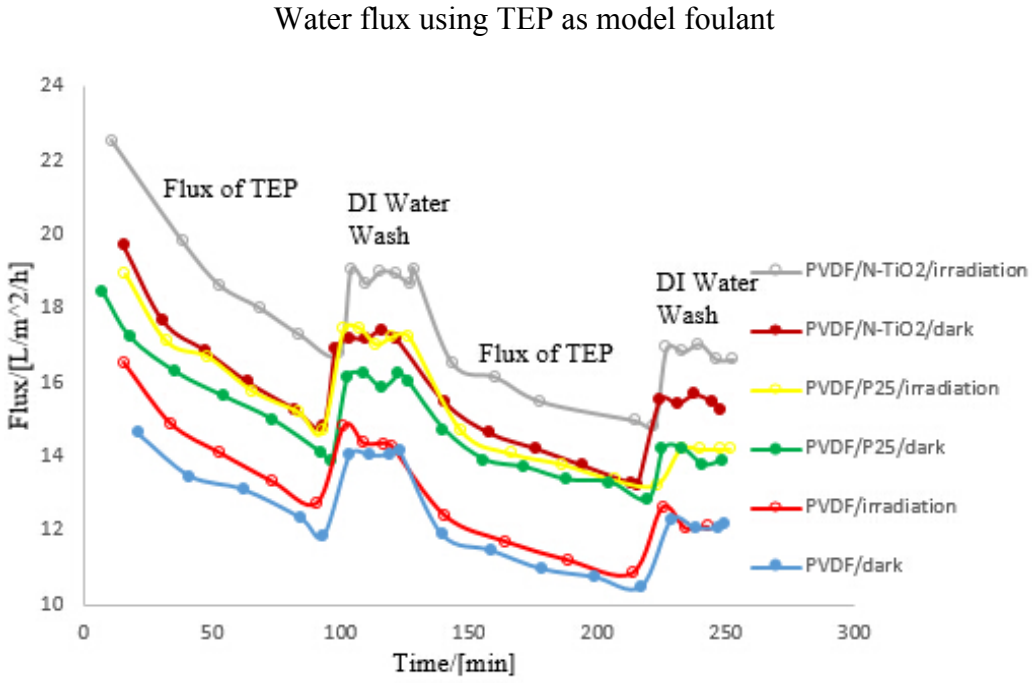

Fig. 15. Fouling behavior of PVDF, PVDF/P25 and PVDF/N-TiO2 memrbanes under dark and visible light irradiation conditions at a constant pressure of 8 psi for 4 h and two cycles with DI water washing.

CHAPTER 4. CONCLUSIONS AND FUTURE STUDIES

4.1 Conclusions

Chlorella Vulgaris had been successfully cultured, and TEPs were seperated from the culture broth. Besides, TEPs were observed and measured by Alcian Blue staining method. A relative value was used in TEP concentration measurement for simplification, and the concentrations of TEP solutions used in evaluating the membrane fouling resistance were controlled to 13~15 abs/cm/L. Size distribution of TEPs in the solution was detected and the average particle size was 2.57 μm, which was within the size range reported in previous studies by others. The zeta potential of TEP solution at pH=7.8 was at -13.3 mV.

During the flux test, flux decrease occurred due to fouling of TEP both in the first and second cycles. After washing the system with DI water during the interval, a new steady state was achieved at a lower initial water flux but higher than the ultimate flux of the first cycle. The system was washed again after the second cycle, and the new steady state was lower than the first one due to irriversible fouling.

By adding TiO_2 nanoparticles into PVDF substrate, the hydrophilicity of the hollow fiber membrane was enhanced, resulting in the increase of pure water flux. This phenomenon was observed for both PVDF/P25 and PVDF/N-TiO_2 membranes. Furthermore, by doping nitrogen into TiO_2 nanoparticles, the photo catalytic properties of nanopartcles were improved by reducing the activation band gap, since for common TiO_2 nanoparticles, the activation band gap is 3.2 eV, which can only be activated by UV light,

while for the N-TiO_2 nanoparticles, it was reduced so that visible light is capable of activating it. Hydrophilicity of N-TiO_2 nanoparticles was further enhanced with visible light irradiation, which contributed to the high pure water flux through PVDF/N-TiO_2 membrane. Hydrophilicities of the membranes were evaluated by measuring contact angles, the results were consistent with the pure water flux tests. Also it had been found that the water flux and fouling resistance of PVDF/N-TiO_2 were improved by visible light irradiation. Characterization of hollow fiber membranes was carried out by using SEM, the nanoparticles were observed uniformly dispersed into the polymer substrate. The rejections of TEP for all membranes were high, while the solute rejections of PVDF/P25 and PVDF/N-TiO_2 were a little lower than the original PVDF membrane. In summary, the PVDF/TiO_2 mixed matrix hollow fiber membrane with visible light irradiation can be successfully applied to ultra filtration due to its excellent hydrophilicity, high fouling resistance and low energy requirement.

4.2 Future studies

Follow-up studies mainly include two parts, one is a more comprehensive research on TEPs and the other is the enhancement and commercial application of hollow fiber membranes.

For the TEP part, future studies should be carried out focusing on the biofilm formation process on membrane surface. The process can be observed at real time to get a better overview of biofilm formation. Furthermore, TEPs can be separated further by size using filter paper with pore sizes of 0.1 μm, 0.2 μm and 0.4 μm, then the fouling

effect of c-TEP and p-TEP can be studied separately. Besides, the chemical and physical properties such as stickness, composition and hydrophilicity of TEP can be studied.

It has been attractive to apply nanotechnologies to membrane fabrication in recent years, lots of scientists and researchers have paid their efforts to innovative modifications of traditional polymer membranes by introducing variaties of nanomaterials. However, development of novel UF membranes with nanotechnology is still at the initial stage, there are still many challenges to break through such as how to cut down the cost of nanomaterial synthesis, how to reduce the energy requirement for both nanomaterial activation and filtration driving force, and how to scale up the filtration systems and make it commercial applicable. For this research, selection of membrane fabrication conditions and formulas is essential for the performance no matter in permeability or fouling resistance, more attempt should be given to get the best performance, which means the membrane with highest permeability and fouling resistance at a reasonable rejection. For example, the size of nanoparticle has great effect on the membrane performance, how to avoid agglomeration when disperse the particles into substrate is important to maintain a high permeability. For all membrane applications, fouling is still a critical issue, improvement of fouling resistance and extending of membrane lifetime is still the main focus for all researches in this field.

BIBLIOGRAPHY

Ahmad, A. L., et al. (2011). "Functionalized PSf/SiO2 nanocomposite membrane for oil-in-water emulsion separation." Desalination **268**(1–3): 266-269.

Alldredge, A. L., et al. (1993). "The abundance and significance of a class of large, transparent organic particles in the ocean." Deep Sea Research Part I: Oceanographic Research Papers **40**(6): 1131-1140.

Berman, T. and M. Holenberg (2005). "Don't fall foul of biofilm through high TEP levels." Filtration & Separation **42**(4): 30-32.

Berman, T. P., Uta (2007). " Transparent Exopolymer Particles (TEP): an overlooked factor in the process of biofilm formation in aquatic environments." Nature, preceedings.

Bessiere, Y., et al. (2005). "Low fouling conditions in dead-end filtration: Evidence for a critical filtered volume and interpretation using critical osmotic pressure." Journal of Membrane Science **264**(1–2): 37-47.

Bilad, M. R., et al. (2012). "Harvesting microalgal biomass using submerged microfiltration membranes." Bioresour Technol **111**: 343-352.

Bourgeous, K. N., et al. (2001). "Ultrafiltration of wastewater: effects of particles, mode of operation, and backwash effectiveness." Water Research **35**(1): 77-90.

Chen, J., et al. (2011). Membrane Separation: Basics and Applications. Membrane and Desalination Technologies. L. Wang, J. Chen, Y.-T. Hung and N. Shammas, Humana Press. **13:** 271-332.

Chen, X. and S. S. Mao (2007). "Titanium Dioxide Nanomaterials: Synthesis, Properties, Modifications, and Applications." Chemical Reviews **107**(7): 2891--2959.

Discart, V., et al. (2013). "Role of transparent exopolymeric particles in membrane fouling: Chlorella vulgaris broth filtration." Bioresource technology **129**: 18-25.

Discart, V., et al. (2013). "Role of transparent exopolymeric particles in membrane fouling: Chlorella vulgaris broth filtration." Bioresour Technol **129**: 18-25.

Discart, V., et al. (2013). "Role of transparent exopolymeric particles in membrane fouling: Chlorella vulgaris broth filtration." Bioresour Technol **129**(0): 18-25.

Engel, A. (1998). Bildung, Zusammensetzung und Sinkgeschwindigkeiten mariner Aggregate. Institut für Meereskunde. Kiel, Germany, Christian-Albrechts-Universität Kiel. **Doctoral thesis/PhD:** 145.

Engel, A. (2000). "The role of transparent exopolymer particles (TEP) in the increase in apparent particle stickiness (alpha) during the decline of a diatom bloom." Journal of Plankton Research **22**(3): 485-497.

Engel, A. and U. Passow (2001). " Carbon and nitrogen content of transparent exopolymer particles (TEP) in relation to their Alcian Blue adsorption." Marine Ecology Progress Series **219**: 1-10.

Escobar, I. C. (2004). "Effects of water chemistries and properties of membrane on the performance and fouling—a model development study." Journal of Membrane Science **238**(1–2).

Fane, A. G., et al. (2011). Membrane Technology: Past, Present and Future. Membrane and Desalination Technologies. L. Wang, J. Chen, Y.-T. Hung and N. Shammas, Humana Press. **13:** 1-45.

Ghosh, A. K. and P. Bandyopadhyay (2012). Polysaccharide-Protein Interactions and Their Relevance in Food Colloids.

Guo, H., et al. (2010). "Low-pressure membrane integrity tests for drinking water treatment: A review." Water Research **44**(1): 41-57.

Guo, X., et al. (2009). "Study on ultrafiltration for surface water by a polyvinylchloride hollow fiber membrane." Desalination **238**(1–3): 183-191.

Hans-Peter Grossart, M. S. (1997). "Formation of macroscopic organic aggregates (lake snow) in a large lake: The significance of transparent exopolymer particles, phytoplankton, and zooplankton." LIMNOLOGY AND OCEANOGRAPHY **42**(8).

Hoagland, K. D., et al. (1993). "DIATOM EXTRACELLULAR POLYMERIC SUBSTANCES: FUNCTION, FINE STRUCTURE, CHEMISTRY, AND PHYSIOLOGY." Journal of Phycology **29**(5): 537-566.

Holman, S. R. and K. N. Ohlinger (2007). "An Evaluation of Fouling Potential and Methods to Control Fouling in Microfiltration Membranes for Secondary Wastewater Effluent." Proceedings of the Water Environment Federation **2007**(11): 6417-6444.

J.C. Schippers, L. V., R. Schurer, H. Winters, G. Amy, M. D. Kennedy (2008). "Membrane fouling potential of transparent exopolymer particles (TEP) from bloom-forming algae."

Jacquet, S., et al. (2005). "The proliferation of the toxic cyanobacterium Planktothrix rubescens following restoration of the largest natural French lake (Lac du Bourget)." Harmful Algae **4**(4): 651-672.

Katsoufidou, K., et al. (2005). "A study of ultrafiltration membrane fouling by humic acids and flux recovery by backwashing: Experiments and modeling." Journal of Membrane Science **266**(1–2): 40-50.

Kennedy, M. D., et al. (2008). Water Treatment by Microfiltration and Ultrafiltration. Advanced Membrane Technology and Applications, John Wiley & Sons, Inc.**:** 131-170.

Kumar M, A. S., Pearce WR. (2006). "Investigation of seawater reverse osmosis fouling and its relationship to pretreatment type." Environ.Sci **Technol. 40**: 2037-2044.

Lee, D.-J., et al. (2012). "Coagulation-membrane filtration of Chlorella vulgaris." Bioresource technology **108**(0): 184-189.

Logan, B. E., et al. (1994). "Direct observation of phytoplankton, TEP and aggregates on polycarbonate filters using brightfield microscopy." Journal of Plankton Research **16**(12): 1811-1815.

Loreen O. Villacorte, R. S., Maria D. Kennedy, Gary L. Amy, and Jan C. Schippers (2010). "Removal and Deposition of Transparent Exopolymer Particles in a Seawater UF-RO System." IDA Journal **2**(1).

Mallick, N., et al. (2012). "Green microalga Chlorella vulgaris as a potential feedstock for biodiesel." Journal of Chemical Technology & Biotechnology **87**(1): 137-145.

Mills, A. and S. Le Hunte (1997). "An overview of semiconductor photocatalysis." Journal of Photochemistry and Photobiology A: Chemistry **108**(1): 1-35.

Mopper, K., et al. (1992). "Determination of sugars in unconcentrated seawater and other natural waters by liquid chromatography and pulsed amperometric detection." Environ Sci Technol **26**(1): 133-138.

Mopper, K., et al. (1995). "The role of surface-active carbohydrates in the flocculation of a diatom bloom in a mesocosm." Deep Sea Research Part II: Topical Studies in Oceanography **42**(1): 47-73.

Mukiibi, M., Feathers, R., &Mukiibi, B. M. (2009). "Membrane Technology : A Breakthrough in Water Treatment." Water Conditioning & Purification.

Nakatsuka, S., et al. (1996). "Drinking water treatment by using ultrafiltration hollow fiber membranes." Desalination **106**(1–3): 55-61.

Passow, U. (2000). "Formation of Transparent Exopolymer Particles, TEP, from dissolved precursor material." Marine ecology-progress series: 1-11.

Passow, U. (2001). " Origin of transparent exopolymer particles (TEP) and their role in the sedimentation of particulate matter." Continental shelf research **21**: 327-346.

Passow, U. (2002). "Transparent exopolymer particles (TEP) in aquatic environments." Progress in Oceanography **55**(3–4): 287-333.

Passow, U. and A. L. Alldredge (1995). "Aggregation of a diatom bloom in a mesocosm: The role of transparent exopolymer particles (TEP)." Deep Sea Research Part II: Topical Studies in Oceanography **42**(1): 99-109.

Paz, Y. (2010). "Application of TiO2 photocatalysis for air treatment: Patents' overview." Applied Catalysis B: Environmental **99**(3–4): 448-460.

Ramus, J. (1977). "ALCIAN BLUE: A QUANTITATIVE AQUEOUS ASSAY FOR ALGAL ACID AND SULFATED POLYSACCHARIDES1." Journal of Phycology **13**(4): 345-348.

Redfield, A. C., et al. (1963). The influence of organisms on the composition of sea-water. London, Intersicence.

Rosdianah Ramli, N. B. and A. Z. Yasser (2002). REVIEW ON THE FACTORS AFFECTING ULTRAFILTRATION HOLLOW FIBER MEMBRANE OPERATIONAL PERFORMANCE IN WATER TREATMENT.

Sangpour, P., et al. (2010). "Photoenhanced Degradation of Methylene Blue on Cosputtered M:TiO2 (M = Au, Ag, Cu) Nanocomposite Systems: A Comparative Study." The Journal of Physical Chemistry C **114**(33): 13955-13961.

Tchobanoglous, G., et al. (2003). Wastewater Engineering: Treatment and Reuse, McGraw-Hill Education.

Vera, L. (2000). "Enhancing microfiltration through an inorganic tubular membrane by gas sparging." Journal of Membrane Science **165**(1).

Villacorte, L. O., et al. (2009). "The fate of Transparent Exopolymer Particles (TEP) in integrated membrane systems: removal through pre-treatment processes and deposition on reverse osmosis membranes." Water Research (Oxford) **43**(20): 5039-5052.

Villacorte, L. O., et al. (2010). "Removal and Deposition of Transparent Exopolymer Particles in a Seawater UF-RO System." IDA Journal of Desalination and Water Reuse **2**(1): 45-55.

Wagner, J. (2001). Membrane Filtration Handbook: Practical Tips and Hints, Osmonics.

Wang, Z., et al. (2005). "Photocatalytic degradation of phenol in aqueous nitrogen-doped TiO2 suspensions with various light sources." Applied Catalysis B: Environmental **57**(3): 223-231.

Xia, S., et al. (2004). "Study of reservoir water treatment by ultrafiltration for drinking water production." Desalination **167**(0): 23-26.

Xu, A.-W., et al. (2002). "The Preparation, Characterization, and their Photocatalytic Activities of Rare-Earth-Doped TiO2 Nanoparticles." Journal of Catalysis **207**(2): 151-157.

Yin, J., et al. (2013). "Multi-walled carbon nanotubes (MWNTs)/polysulfone (PSU) mixed matrix hollow fiber membranes for enhanced water treatment." Journal of Membrane Science **437**(0): 237-248.

Zhang, Q. and C. D. Vecitis (2014). "Conductive CNT-PVDF membrane for capacitive organic fouling reduction." Journal of Membrane Science **459**(0): 143-156.